

SDC-90-00067

DT
T

SDC
SOLENOIDAL DETECTOR NOTES

**HIGH P_t FORWARD RAPIDITY TRACKING TRIGGER
USING SILICON PLANES**

John A.J. Matthews

August 1990

High P_t Forward Rapidity Tracking Trigger Using Silicon Planes

John A.J. Matthews
Johns Hopkins University
Baltimore, MD 21218

August 1990

1. Introduction

Tracking information is an important input to lepton and isolated photon triggers at pp and $p\bar{p}$ colliders. In solenoid detectors such as SDC, high P_t tracking triggers are designed to find tracks with limited curvature in the plane perpendicular to the magnetic field direction. This is relatively easy for the central values of rapidity, $|\eta| < 1.5$, where there are axial tracking systems, but this has been difficult for forward rapidities. However with silicon planes that directly measure track azimuth at different locations along the beam/magnetic field direction, high P_t tracking triggers are also relatively easy for forward rapidities. For the SDC silicon tracker geometry^[1] presented in this note the forward tracking trigger covers the range $1.2 < |\eta| < 2.5$.

The outline of this note is as follows. In Section 2, we review the equations for charged tracks in the solenoid, and discuss one approach to select high P_t tracks in both central and forward rapidity regions. A simple algorithm for finding high P_t tracks in the SDC forward silicon planes is presented in Section 3, and simulation results are shown for single tracks. Section 4 gives the trigger efficiency in 800 GeV Higgs events where $Higgs \rightarrow ZZ \rightarrow e^+e^-\mu^+\mu^-$. Finally Section 5 provides a summary and brief discussion of suggested future studies.

2. High P_t Tracking Triggers

In a solenoid geometry with the magnetic field along the z axis, the helical motion for a charged track starting from the origin can be described by:

$$r = 2\rho \sin(\phi_0 - \phi)$$

$$z = 2\rho(\phi_0 - \phi)\tan\lambda + z_0$$

where r is the radial distance of the track from the beam line, z is the distance along the beam line from the nominal beam interaction point, z_0 is the actual z location of the interaction

point, ϕ is the azimuth of the track at (r, z) , ϕ_0 is the initial track azimuth at the origin, r is the track radius of curvature in the x, y plane, and $\tan\lambda$ is the tangent of the dip angle, λ . Alternatively $\tan\lambda$ is given by the cotangent of the angle of the track to the beam direction. It is convenient to define the track curvature, $\kappa \equiv \frac{1}{2\rho}$, which is then related to the magnetic field, B , and the track P_t :

$$\kappa = \frac{0.3B}{2P_t}$$

where κ is in m^{-1} , B is in Tesla, and P_t is in GeV/c.

Differentiating the track equations above gives for the central region:

$$\kappa = \frac{-(\frac{d\phi}{dr})}{\sqrt{1 + (r\frac{d\phi}{dr})^2}} \approx -(\frac{d\phi}{dr})$$

and for the forward region:

$$\kappa = -(\frac{d\phi}{dz}) \tan\lambda$$

For high P_t tracks, $\kappa \ll 1$; thus high P_t tracks are characterized by small values of $(\frac{d\phi}{dr})$ or $(\frac{d\phi}{dz})$:

$$(\frac{d\phi}{dr}) \approx -\kappa = (\frac{0.3B}{2P_t})$$

$$(\frac{d\phi}{dz}) = -\frac{\kappa}{\tan\lambda} = (\frac{0.3B}{2P_t}) \frac{1}{\tan\lambda}$$

This characteristic could be used to selecting high P_t tracks in the tracking system. As an example, to accept tracks with $P_t > P_{t,threshold}$ for central values of rapidity, one possible trigger could require that $|(\frac{d\phi}{dr})| < (\frac{d\phi}{dr})_{threshold}$:

$$(\frac{d\phi}{dr})_{threshold} = (\frac{0.3B}{2P_{t,threshold}})$$

For forward rapidities the relevant quantity is $(\frac{d\phi}{dz}) = (\frac{d\phi}{dr}) \frac{1}{\tan\lambda}$. A high P_t trigger could require that $|(\frac{d\phi}{dz})| < (\frac{d\phi}{dz})_{threshold}$:

$$\left(\frac{d\phi}{dz}\right)_{\text{threshold}} = \left(\frac{0.3B}{2P_{t,\text{threshold}}}\right) \frac{1}{\tan\lambda}$$

where $\tan\lambda$ is defined by the geometry of the forward silicon planes.

Thus a possible high P_t trigger would select tracks with small $(\frac{d\phi}{dr})$ or $(\frac{d\phi}{dz})$. An algorithm to find these tracks could be a simple search for a minimum number of hits in the tracking system in roads of limited azimuthal width, $\Delta\phi$:

$$\Delta\phi = \pm\left(\frac{d\phi}{dr}\right) \Delta r = \pm\left(\frac{d\phi}{dz}\right) \Delta z$$

To obtain a feeling for the magnitude of the different quantities consider the SDC silicon tracker. The magnetic field is 2 Tesla, and the silicon tracker has dimensions: $r_{\text{inner}} = 0.15$ m and $r_{\text{outer}} = 0.54$ m. For a threshold $P_t = 10$ GeV/c: $\kappa = 0.03$ m⁻¹, $\Delta\phi < \pm 12$ mrad, and the track spatial offset between inner and outer radii is $r_{\text{outer}}\Delta\phi < \pm 6.5$ mm. In practice a simple search procedure using a single $\Delta\phi$ road is adequate only for large P_t thresholds. For $P_t \sim 10$ GeV/c it is probably essential to use a number of P_t bins so that $\Delta\phi$ is limited to a few milli-radians. For example P_t thresholds of 10, 13.33, 20, and 40 GeV/c would provide equal $\Delta\phi$ bins of width $\sim \pm 3$ milli-radians in the SDC silicon tracker.

To illustrate this further, Fig. 1 shows the hits in a possible SDC tracking system from a single 800 GeV Higgs event, where the Higgs decays into $2Z$ s, and the Z s decay into lepton pairs. The quarter section of the tracking elements is shown in Fig. 2. Fig. 1a shows the hits in the axial tracking elements, and Fig. 1b shows the hits in the forward silicon planes. For the axial trackers an $x - y$ view of the event and a $\phi - r$ view are shown; for the forward planes only the $\phi - z$ view is shown. The leptons from the Z decays are also shown separately. As discussed above, since these tracks are at high P_t they are essentially vertical lines in the respective $\phi - r$ or $\phi - z$ plots; in contrast to this the more numerous low P_t tracks have large slopes. Thus a trigger limiting $(\frac{d\phi}{dr})$ or $(\frac{d\phi}{dz})$ would select the high P_t leptons and be insensitive to low P_t backgrounds. However even isolated high P_t leptons often cross lower momentum tracks, thus triggers can not be too simplistic.

3. High P_t Forward Rapidity Tracking Trigger

As discussed in Section 2, triggering on high P_t tracks at forward rapidities is conceptually the same as for central rapidities. The trigger searches for track candidates that satisfy $|\left(\frac{d\phi}{dz}\right)| < \frac{0.3B}{2P_{t,\text{threshold}} \tan\lambda}$ where for the forward silicon planes $\tan\lambda$ is given by the geometry of the detector planes (tracking superlayers), see Fig. 3. To a good approximation:

$$\frac{1}{\tan\lambda} \sim \frac{r_{\text{outer}}}{z_{\text{max}}}$$

where r_{outer} is the outer radius of the tracking superlayer (pairs of silicon planes form tracking superlayers) at the largest z_{max} that contains a given track candidate.

Thus:

$$\left(\frac{d\phi}{dz}\right) < \left(\frac{d\phi}{dz}\right)_{\text{threshold}} = \left(\frac{0.3B}{2P_{t\text{threshold}}}\right)\left(\frac{r_{\text{outer}}}{z_{\text{max}}}\right)$$

and high P_t tracks can be identified by having at least a minimum number of hits in a limited $\Delta\phi$ road of width:

$$\Delta\phi = \pm\left(\frac{0.3B}{2P_{t\text{threshold}}}\right)\left(\frac{r_{\text{outer}}}{z_{\text{max}}}\right)\Delta z$$

where Δz is the length of the track along the beam direction in the forward silicon tracker.

To evaluate the efficacy of this trigger a simple simulation was carried out to evaluate the efficiency and robustness of a single P_t threshold trigger. The trigger simulation used the SDC silicon tracker geometry, Fig. 3, and assumed no cracks/detector inefficiencies. Only the information on the ϕ -strips was used and the $\tan\lambda$ information was provided by the detector geometry. Consequently the stereo-strip information was not required, nor was any information used on the possible radial segmentation of the silicon detectors in a plane. The beauty of the silicon planes was that they provided a measurement of ϕ directly, and that the overall mechanical dimensions were adequate to define $\tan\lambda$. The trigger utilized the natural superlayer grouping of planes to find *track vector* candidates, and required hits on several superlayers to be robust against random combinatoric *fake* triggers.

To form acceptable superlayer track vectors measurements ϕ_1 and ϕ_2 from layers 1 and 2 of a superlayer were required to satisfy:

$$|\phi_1 - \phi_2| < \left(\frac{d\phi}{dz}\right)_{\text{threshold}} |z_1 - z_2|$$

where z_1 and z_2 are the z locations of the two measurement planes. Thus all superlayer track vectors were required to be consistent with the high P_t trigger.

To form acceptable track candidates hits in superlayers were combined as follows. The trigger simulation searched for track vector candidates starting at large $|z|$, and then continuing in to smaller $|z|$. The largest $|z|$ superlayer defined $\tan\lambda$ as discussed above. Track vectors found in this superlayer were denoted *seed* track vectors. Each seed track vector defined a $\Delta\phi$ road used to search for additional track vectors to be added to the track candidate from superlayers closer to the interaction point. Labelling these superlayers with the index k , then track vector hits were added to a track if:

$$| \langle \phi_{\text{seed}} \rangle - \langle \phi_k \rangle | < \left(\frac{d\phi}{dz}\right)_{\text{threshold}} | \langle z_{\text{seed}} \rangle - \langle z_k \rangle |$$

where the $\langle \text{quantity} \rangle$ represents the value determined from the pair of measurements per superlayer. Track candidates were then accepted if they contained a minimum number of hits (typically 7 corresponding to 4 superlayers).

The above procedure was repeated choosing the seed superlayer initially with the largest $|z|$ superlayer, and on subsequent iterations defining the seed superlayer to be the next superlayer closer to the interaction point, and so. To allow for an adequate number of superlayers to define a track, seed superlayers closer than 4 superlayers from the interaction point were not considered. This procedure was done separately for the two *arms* of silicon planes at positive and negative z .

One outcome of this rather simple logic is that high P_t tracks were typically found more than once; that is they were identified as trigger candidates having seed track vectors in different superlayers. These duplicates could be removed, along with a few percent of true second triggers, by rejecting later triggers within ± 5 milli-rad in ϕ of an earlier trigger.

The resulting trigger efficiency as a function of P_t and rapidity, η , are shown in Fig. 4a-c for P_t thresholds of 10, 20 and 40 GeV/c respectively. These results were obtained simulating only a single track in the detector at one time. Tracks were generated uniformly in rapidity between $-2.5 < \eta < 2.5$ and in transverse momentum between $1 < P_t < 100$ GeV/c. The simulation^[2] included multiple scattering in the detectors and estimated support material. In addition the initial track starting point, z_0 , was Gaussianly distributed with a RMS width of 7 cm. The x, y origin of the tracks was set at the tracking system center. In Fig. 4 the efficiency plots of P_t were compiled with the restriction $1.2 < |\eta| < 2.5$ and the efficiency plots for η required $P_t > P_{t,threshold}$. The P_t turn-on of the simple high P_t trigger is satisfactory, and the η coverage is basically the geometrical coverage of the system.

The trigger logic discussed above is based on the assumption that the track originates from the beam line which is also the central axis of the tracking system; that is at $r = 0$. If this is not the case then the track ϕ coordinate measured at tracking radius r is slightly incorrect by an amount (for $b \ll r$):

$$\Delta\phi \sim \frac{b}{r}$$

where b is the impact parameter, see Fig. 5. A finite impact parameter will not effect the high P_t trigger as long as:

$$\Delta\phi_{finite\ b} \ll \Delta\phi_{trigger\ road}$$

This is equivalent to:

$$b \frac{r_{outer} - r_{inner}}{r_{outer}r_{inner}} \ll \left(\frac{0.3B}{2P_{threshold}} \right) (r_{outer} - r_{inner})$$

Thus:

$$b \ll \left(\frac{0.3B}{2P_{\text{threshold}}} \right) r_{\text{outer}} r_{\text{inner}}$$

For the parameters of the SDC silicon tracker:

$$b \ll 1.2\text{mm} \left(\frac{20\text{GeV}/c}{P_{\text{threshold}}} \right)$$

Consequently tracks with impact parameters greater than a few hundred microns are expected to have a reduced trigger efficiency in a silicon tracker based trigger. In addition tracks with a finite impact parameter will cause an increased smearing of the P_t turn-on of the trigger. These effects can be understood from the fact that the ϕ error causes some high P_t tracks to appear more curved, so they fail the trigger, and causes some low P_t tracks to appear less curved, so they pass the trigger. As discussed below, this problem should be limited to the tracks from long lived primary tracks, and/or to beam motion with the monitoring time of the experiment.

To confirm the simple model above, a simulation was done starting tracks uniformly along the x axis between $0 < x < 5\text{mm}$ rather than from the origin. For a $20\text{ GeV}/c$ P_t trigger the efficiency is shown as a function of the starting distance of the track from the origin in Fig. 6. The results are in good agreement with the simple model above.

It is possible to limit the effects of a relative offset of the beam and detector origins by two means: either align the silicon tracking system to the beam, or be prepared to implement a correction for the relative origin offset. To understand how a simple correction can be implemented consider the following. In a rotated geometry where the beam line is located on the rotated silicon detector x axis at x_B , then:

$$(\phi_{\text{observed}} - \phi_{\text{true}}) \sim -\left(\frac{x_B \sin(\phi_0)}{r} \right)$$

where $\sin(\phi_0)$ is the track initial azimuth and the other notation should be clear. For high P_t tracks: $\phi_0 \sim \phi_{\text{observed}}$ and we assume that x_B can be determined from the data and is stable to an adequate precision. Therefore the right hand side of this relation can be determined, and the ϕ measurements have an offset that varies with r and ϕ_0 in a known way. Since $r = \frac{z}{\tan\lambda}$ this also applies to the forward silicon measurements as a function of z .

For the high P_t trigger considered in this note track candidates are selected by requiring $\left(\frac{d\phi}{dr} \right)$ or $\left(\frac{d\phi}{dz} \right)$ to be limited. Therefore it is necessary to determine how a relative origin offset effects the comparison of any two azimuthal measurements, say ϕ_i and ϕ_1 . The result is that when comparing ϕ_1 to ϕ_i , ϕ_1 should be corrected to:

$$\phi_1 \rightarrow \phi_1 + x_B \sin(\phi_0) \left(\frac{1}{r_1} - \frac{1}{r_i} \right)$$

for axial measurements, and for the forward silicon planes ϕ_1 should be corrected to:

$$\phi_1 \rightarrow \phi_1 + x_B \sin(\phi_0) \tan \lambda \left(\frac{1}{z_1} - \frac{1}{z_i} \right)$$

For the silicon trigger simulations the relative beam and silicon origin offset was corrected as follows:

$$\phi_1 \rightarrow \phi_1 + \frac{x_B \sin(\phi_1) z_1}{r_{1_{outer}}} \left(\frac{1}{z_1} - \frac{1}{z_i} \right)$$

where ϕ_1 is a seed track vector; see discussion above. The results of a simulation where the track origin was offset by 2.5 mm from the silicon tracker origin are shown in Fig. 7. With the track offset correction, the trigger efficiency for a 20 GeV/c trigger were essentially the same as in Fig. 4b. Thus the simple correction works adequately. The problem is that even such a simple ϕ correction may be difficult to implement in a low level trigger.

4. Trigger Study with 800 GeV Higgs Events

Although the forward silicon high P_t trigger described above has the capability to trigger on high P_t tracks, extensive simulations are needed to determine its robustness to backgrounds. An initial study has been done with the simulation of 800 GeV Higgs production using Isajet^[3] at SSC energies. The trigger simulation was as described above. The events were tracked through a model of the SDC tracking system, including multiple scattering. Tracks were allowed to loop for a total track length of 50 m.^[2] Minimum-bias event background events are not overlaid on the Higgs events, however to a certain extent the effect of the minimum bias event background was duplicated by allowing the tracks to loop 10-times longer than the detector resolving time.

The results of two simulations are reported here. Both have a trigger P_t threshold set to 20 GeV/c. However in the second simulation an additional *electromagnetic/muon* trigger, with a P_t threshold of 10 GeV/c and limited in rapidity to $1 < |\eta| < 3$, restricted the azimuthal search regions for the silicon tracking trigger. Thus in the first simulation the silicon acts as a stand alone trigger that could function in parallel with high P_t em/muon triggers. In the second simulations the em/muon triggers are assumed to be provided to the silicon tracker from a lower level trigger. In this latter simulation, the silicon data were searched for high P_t triggers in azimuthal regions of ± 100 milli-radians with respect to the azimuth of the em/muon triggers.

The silicon trigger efficiency as a function of track P_t and as a function of track rapidity is shown in Fig. 8, and 9 for simulation 1 and 2 respectively. The results are rather similar to the ideal single track simulations in Section 3. An examination of the figures does show that the efficiencies are slightly higher in Fig. 9 than in Fig. 8. However in Fig. 9 the efficiency is given only for the high P_t leptons, and in Fig. 8 the efficiency is for high P_t leptons and hadrons. Thus it is likely that for isolated tracks the two cases are equivalent, and that the trigger efficiency is reduced in the neighborhood of jets (which contribute to Fig. 8). Finally Fig. 10, and 11 provide some details on the number and makeup of triggers for the two Higgs simulations.

5. Summary

The forward silicon planes proposed for the SDC detector have been shown to have a significant potential for providing high P_t charged particle triggers over the forward regions of rapidity, $1.2 < |\eta| < 2.5$. A simple algorithm to select high P_t tracks was suggested by the track helical motion through the forward silicon detectors. The algorithm was naturally matched with the intrinsic ϕ measurement proposed for these detectors. In addition the information on the track dip angle, or $\tan\lambda$, was adequately provided by the forward silicon superlayer structure. The initial simulations of high P_t triggers on isolated tracks or on tracks in 800 GeV Higgs events resulted in high efficiencies and no large backgrounds from fake triggers.

A number of topics have not yet been investigated. These include applying alternate trigger algorithms to the forward silicon system, changing the high P_t trigger from a single threshold trigger to a trigger that samples in several P_t bins, and detailed studies of how multiple low momentum tracks can fake high P_t triggers. In this regard it is particularly interesting to obtain a quantitative estimate of the immunity to spurious triggers from multiple minimum-bias events that will be part of high luminosity operation of the SSC.

6. References

1. **The Solenoid Detector Experiment**, A. Seiden, Proceedings of the Workshop on Major SSC Detectors, Tucson, AZ, Feb 18-23, P95, (1990);
Silicon Tracking Simulations for the Solenoid Detector Experiment, John A.J. Matthews, Proceedings of the Workshop on Major SSC Detectors, Tucson, AZ, Feb 18-23, P303, (1990)
2. **SILANL - Silicon Tracking System Simulation Program for the SSC**, J. Hylen, J. Matthews, A. Weinstein (1990)
3. **A Monte Carlo Event Generator for pp and $p\bar{p}$ Reactions**, F. Paige and S. Protopopescu

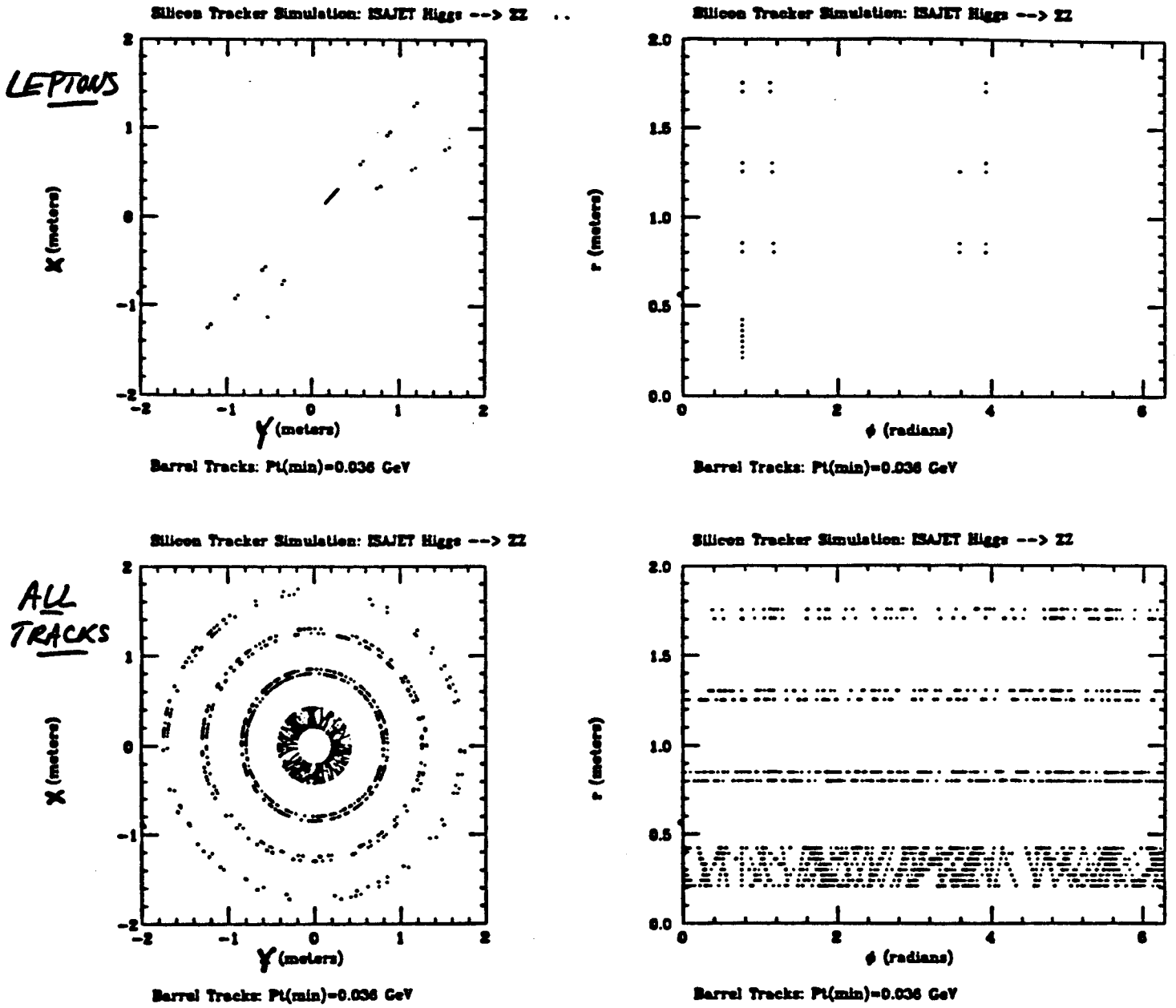
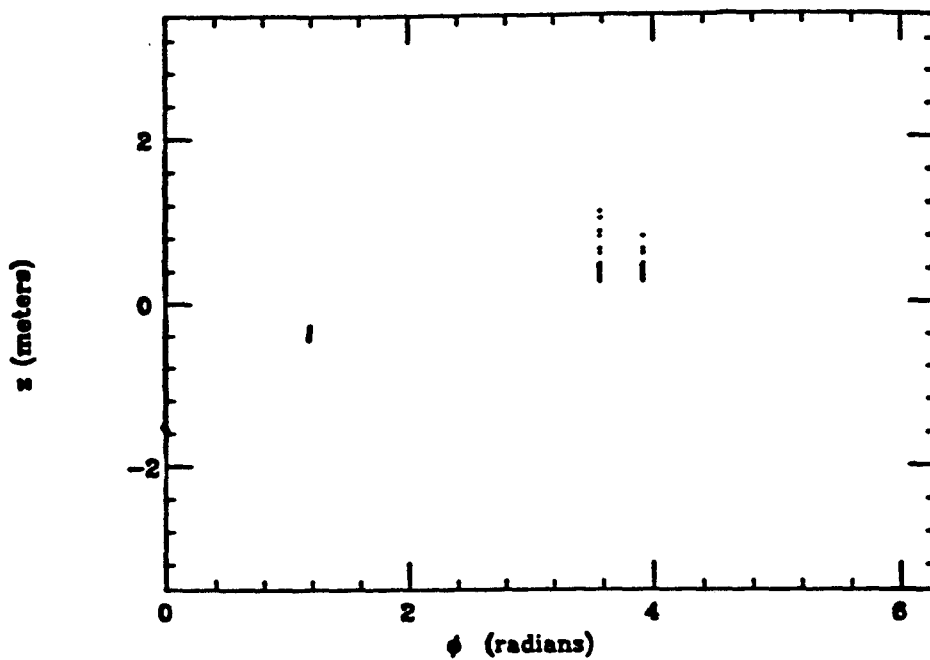


Figure 1a) Hits in a possible SDC tracking system from a 800 GeV Higgs event at the SSC, with the decay $Higgs \rightarrow ZZ \rightarrow e^+e^- \mu^+\mu^-$. Hits are shown from the central axial tracking detectors. The hits are shown in the end or $x - y$ view, and also in the $\phi - r$ view.

Silicon Tracker Simulation: ISAJET Higgs --> ZZ



Forward Tra.

Silicon Tracker Simulation: ISAJET Higgs --> ZZ

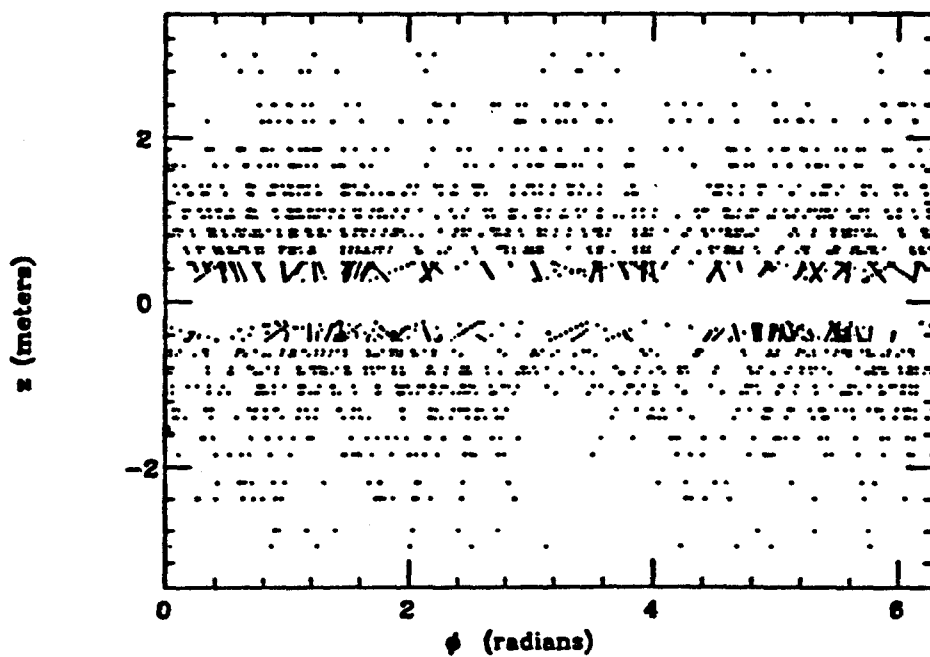


Figure 1b) Hits in a possible SDC tracking system from a 800 GeV Higgs event at the SSC, with the decay $Higgs \rightarrow ZZ \rightarrow e^+e^- \mu^+\mu^-$. Hits are shown from the forward silicon tracking planes. The hits are shown in the natural $\phi - z$ view.

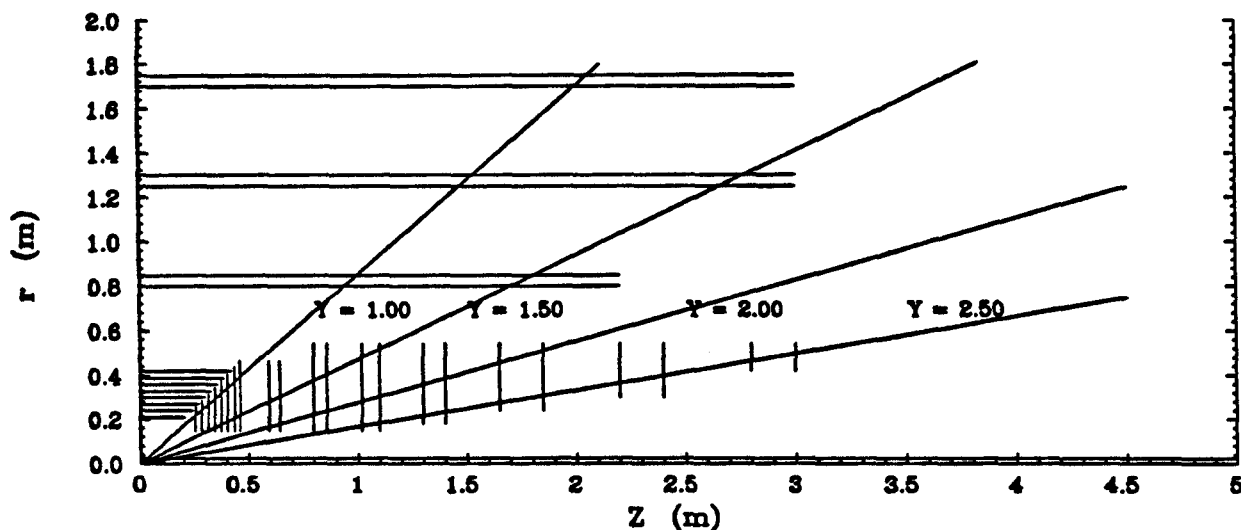


Figure 2 Quarter-section schematic showing a possible SDC tracking system; the lines show various values of rapidity.

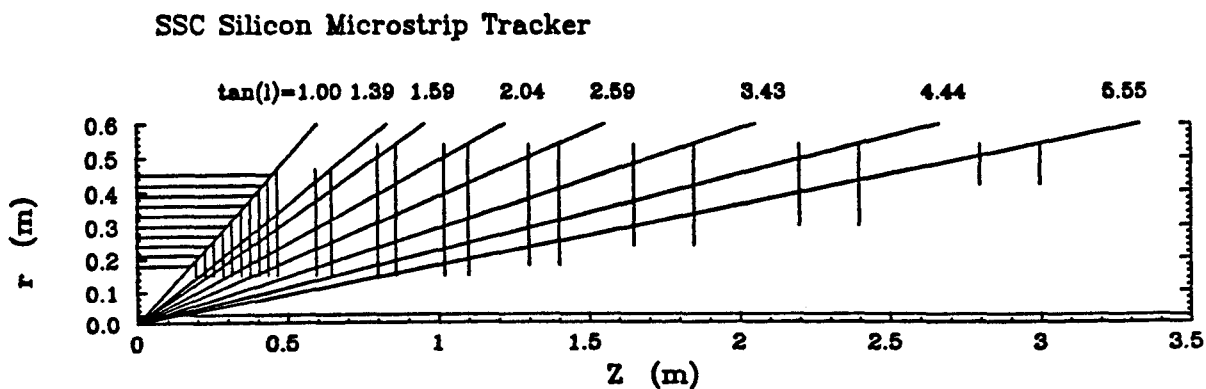


Figure 3 Quarter section schematic showing a possible SDC silicon tracking system; the lines show the $\tan \lambda$ intervals delineated by the forward silicon superlayers.

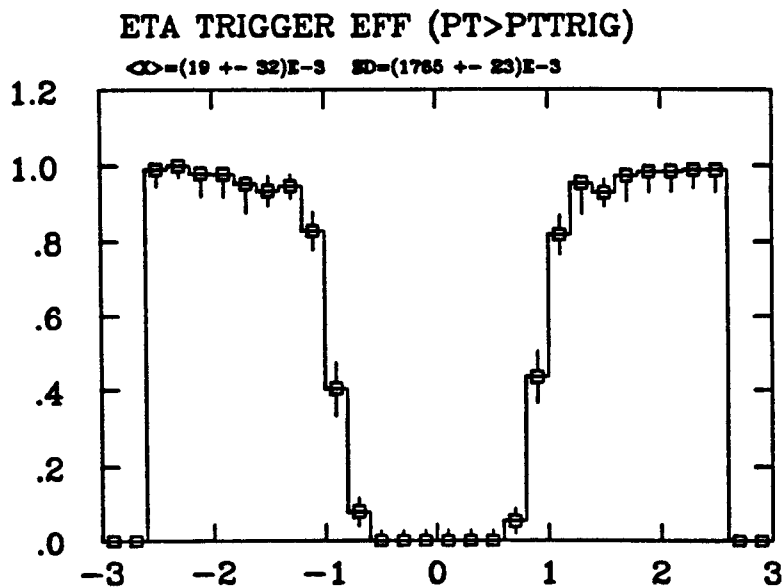
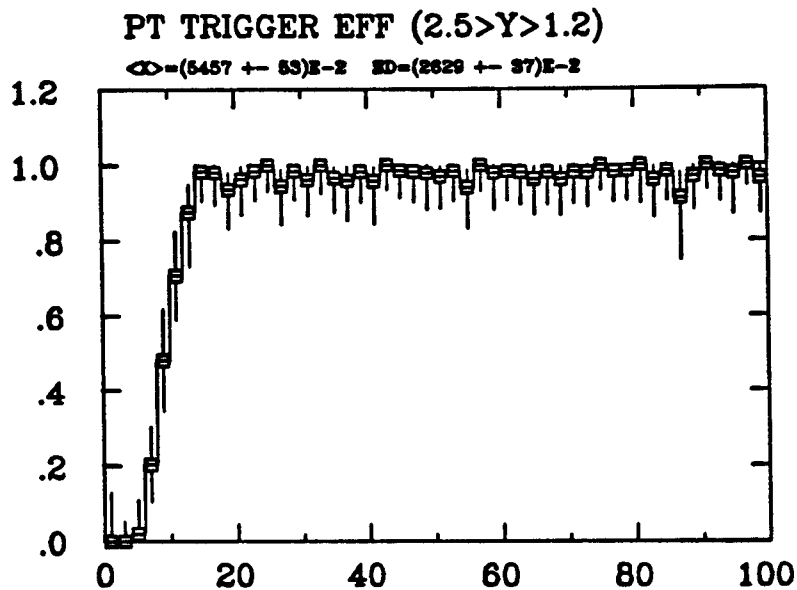


Figure 4a) Forward silicon trigger efficiency as a function of P_t in GeV/c, upper plot, and as a function of rapidity, lower plot, for a P_t threshold of 10 GeV/c.

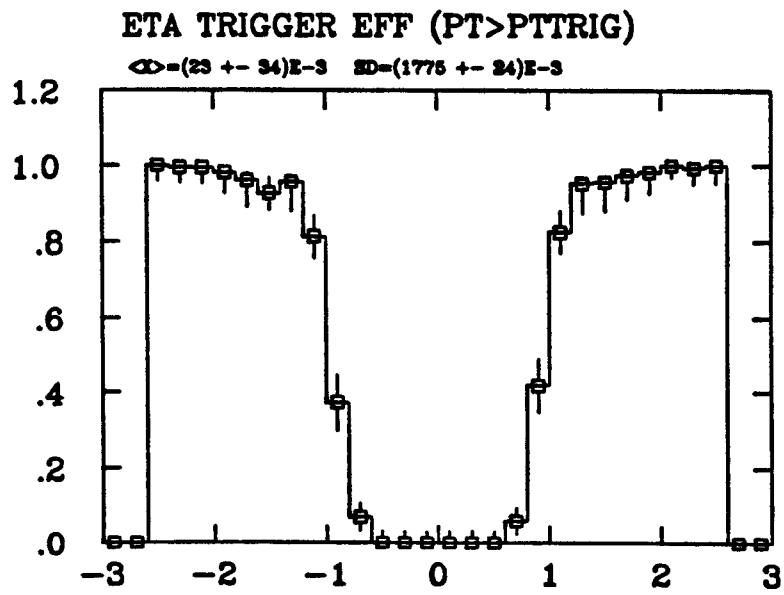
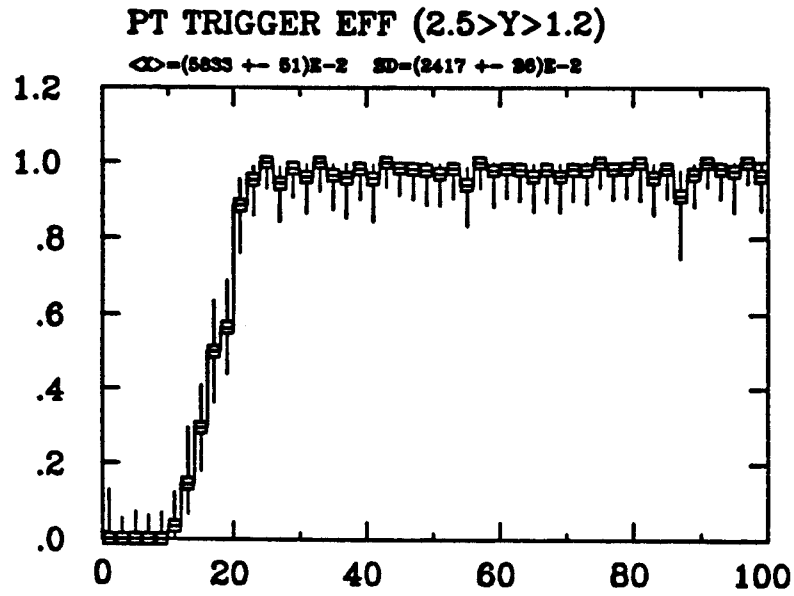


Figure 4b) Forward silicon trigger efficiency as a function of P_T in GeV/c, upper plot, and as a function of rapidity, lower plot, for a P_T threshold of 20 GeV/c.

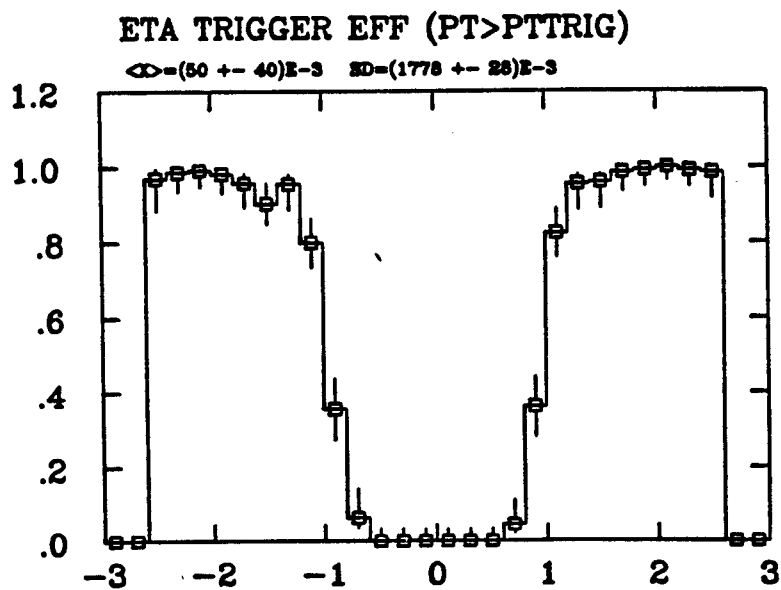
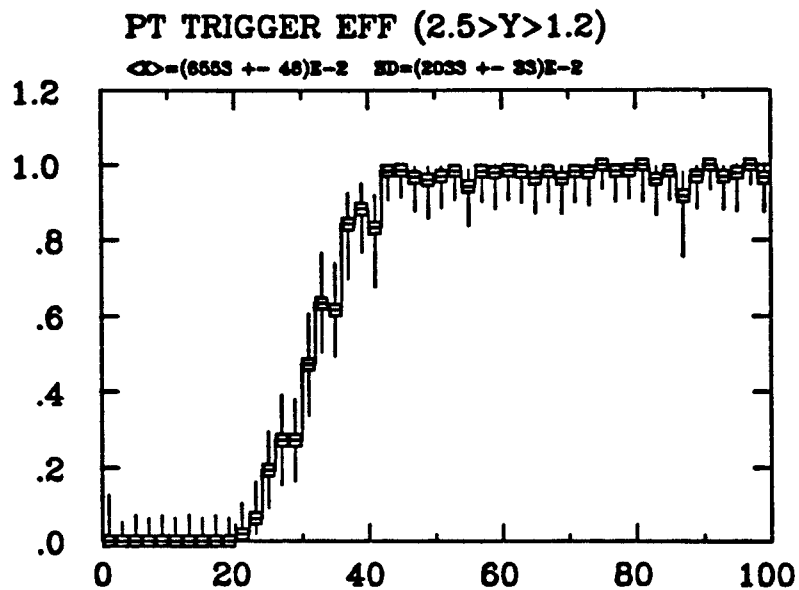


Figure 4c) Forward silicon trigger efficiency as a function of P_t in GeV/c, upper plot, and as a function of rapidity, lower plot, for a P_t threshold of 40 GeV/c.

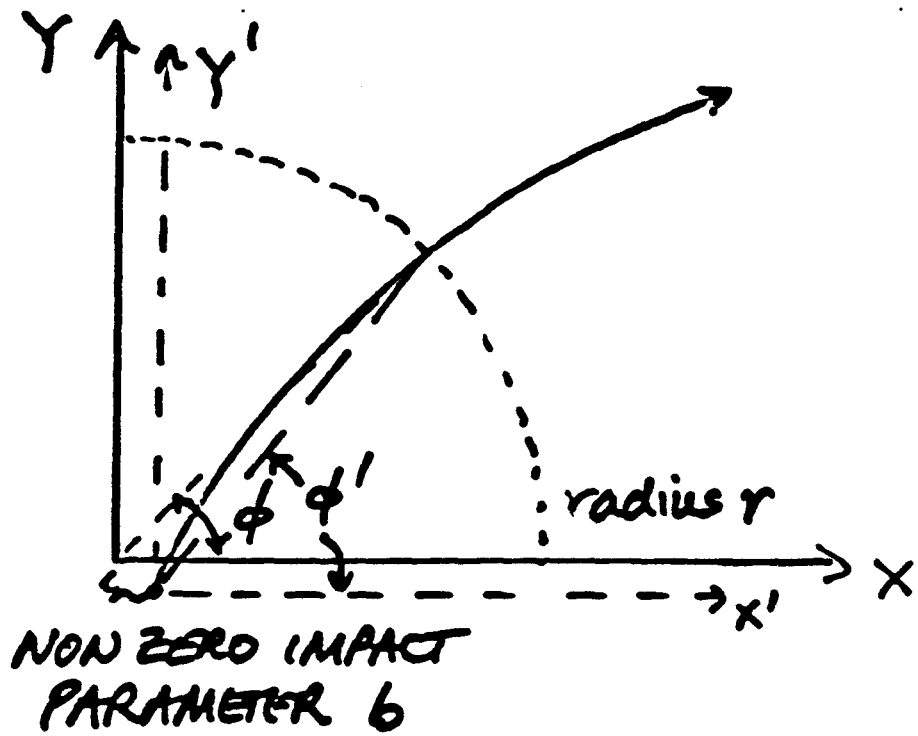


Figure 5 Sketch showing that $\phi = \phi_{observed}$ differs from $\phi' = \phi_{actual}$ for tracks that have a non-zero impact parameter, b .

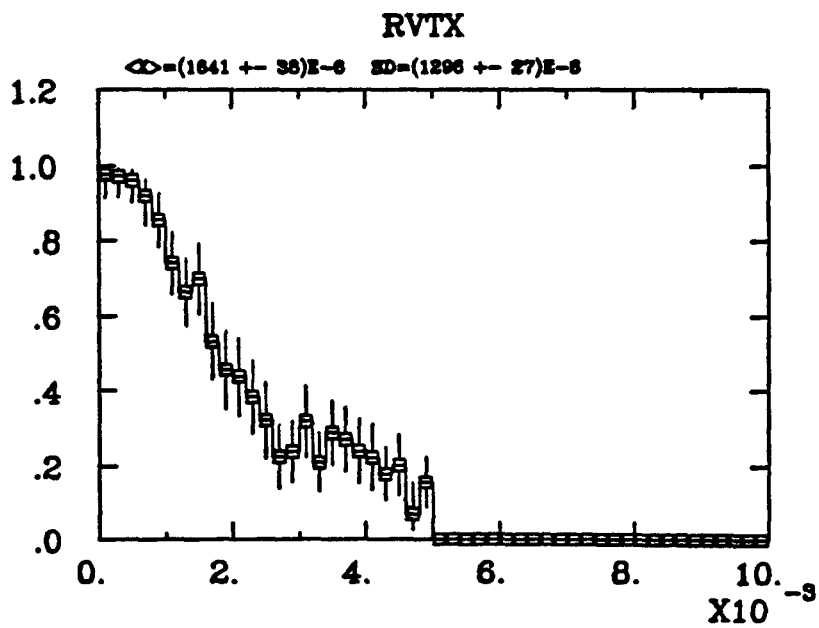


Figure 6 Forward silicon trigger efficiency as a function of the track starting distance from the origin of the silicon tracker coordinates. The horizontal scale is in meters. Tracks were generated uniformly in the interval $0 < x < 5$ mm.

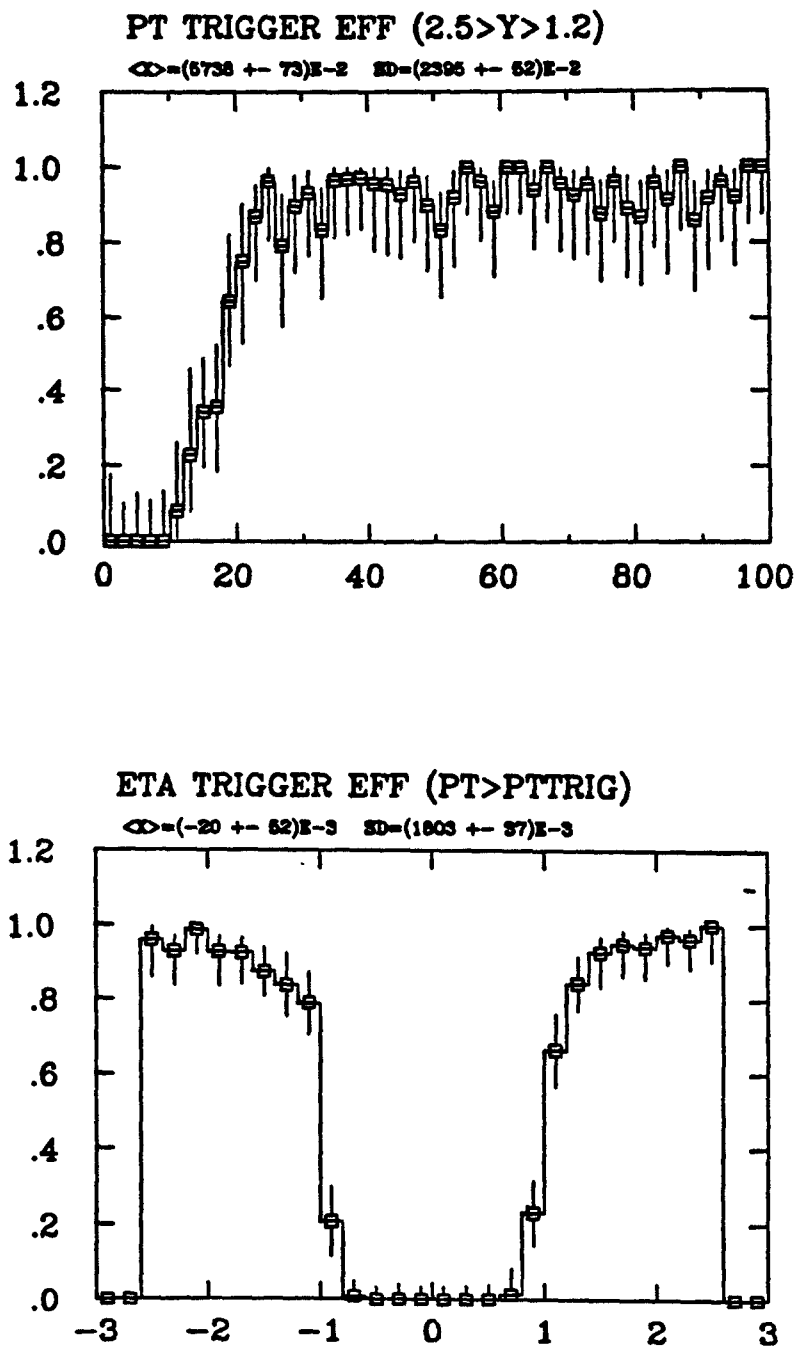


Figure 7 Forward silicon trigger efficiency as a function of P_t in GeV/c, upper plot, and as a function of rapidity, lower plot, for a P_t threshold of 20 GeV/c. All tracks for this simulation started at $(x, y) = (2.5, 0.0)$ mm rather than at $(0, 0)$.

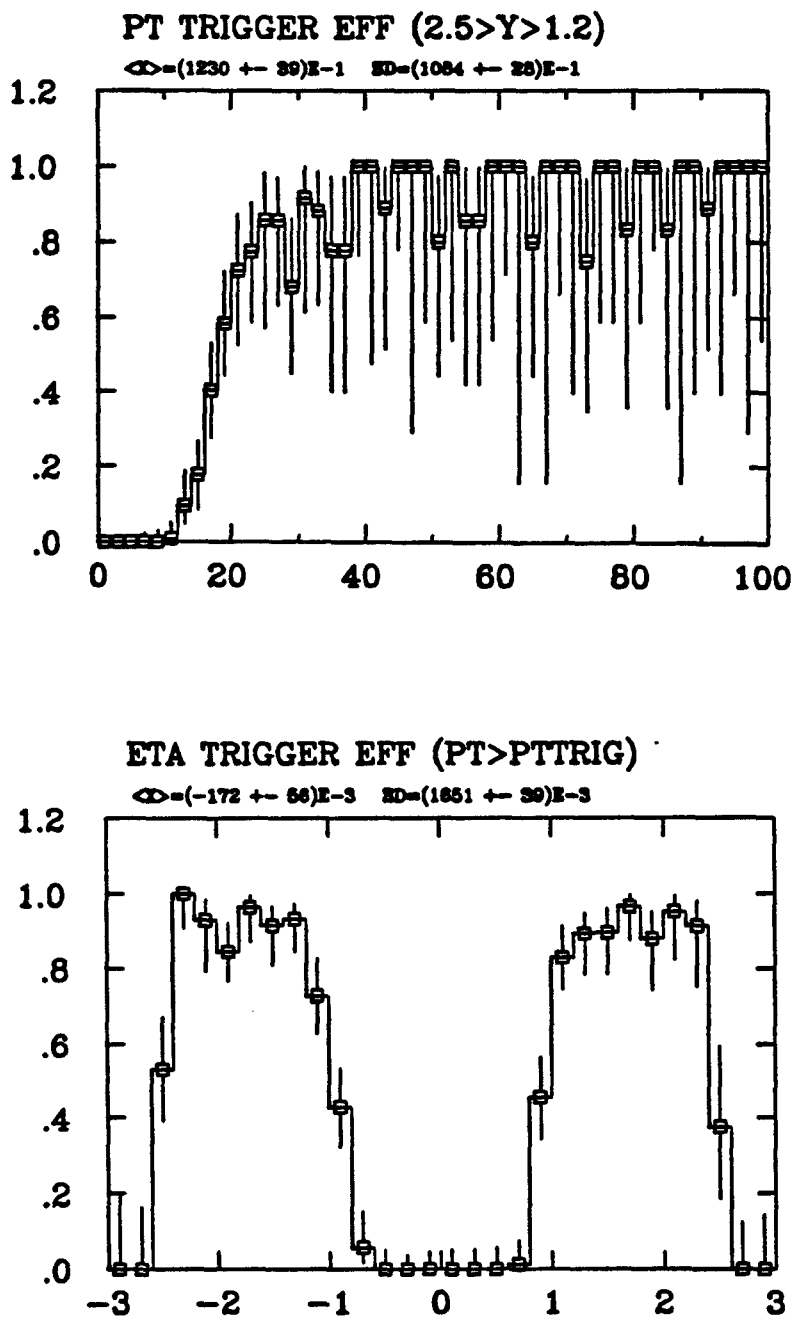


Figure 8 Forward silicon trigger efficiency as a function of P_t in GeV/c, upper plot, and as a function of rapidity, lower plot, with a P_t threshold of 20 GeV/c for 800 GeV Higgs events at the SSC.

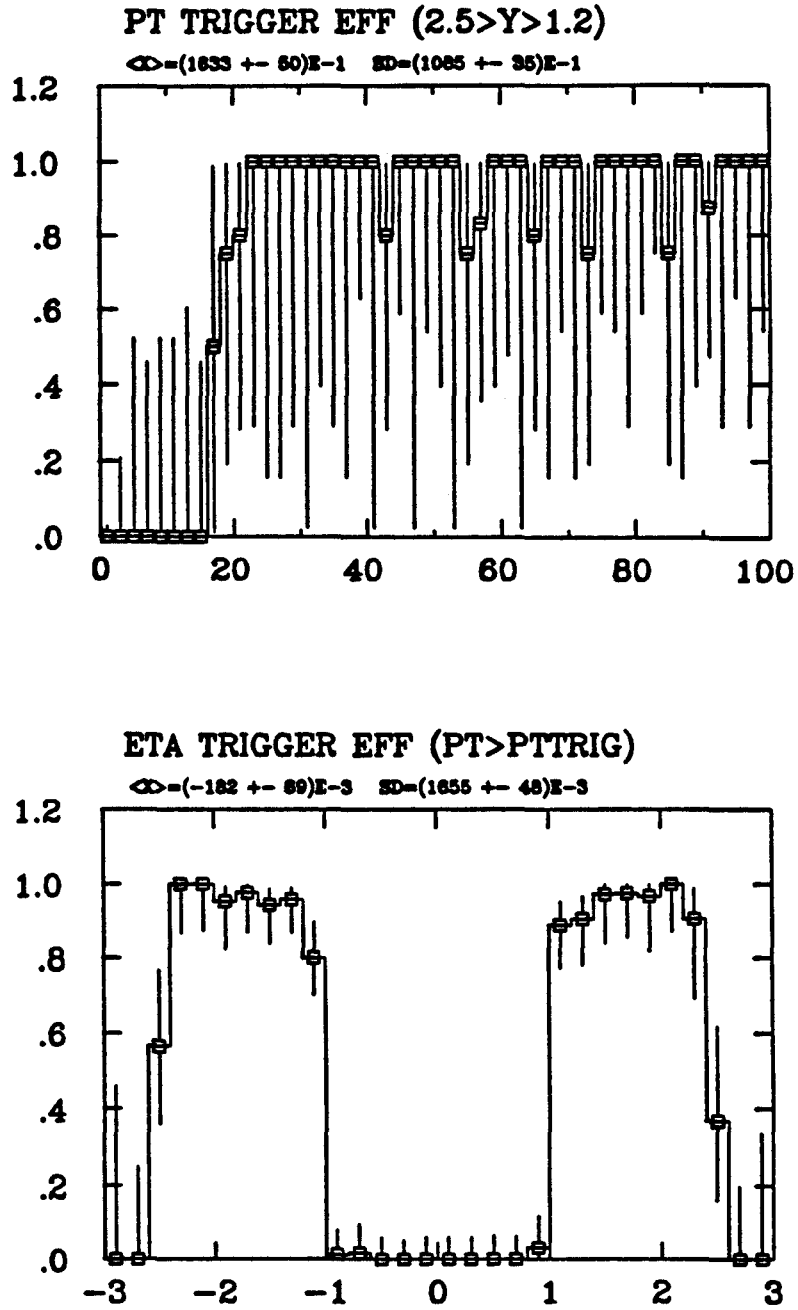


Figure 9 Forward silicon trigger efficiency as a function of P_t in GeV/c, upper plot, and as a function of rapidity, lower plot, with a P_t threshold of 20 GeV/c for 800 GeV Higgs events at the SSC. For this simulation the silicon triggers were required to be within ± 100 mrad of 10 GeV/c P_t threshold electromagnetic/muon triggers.

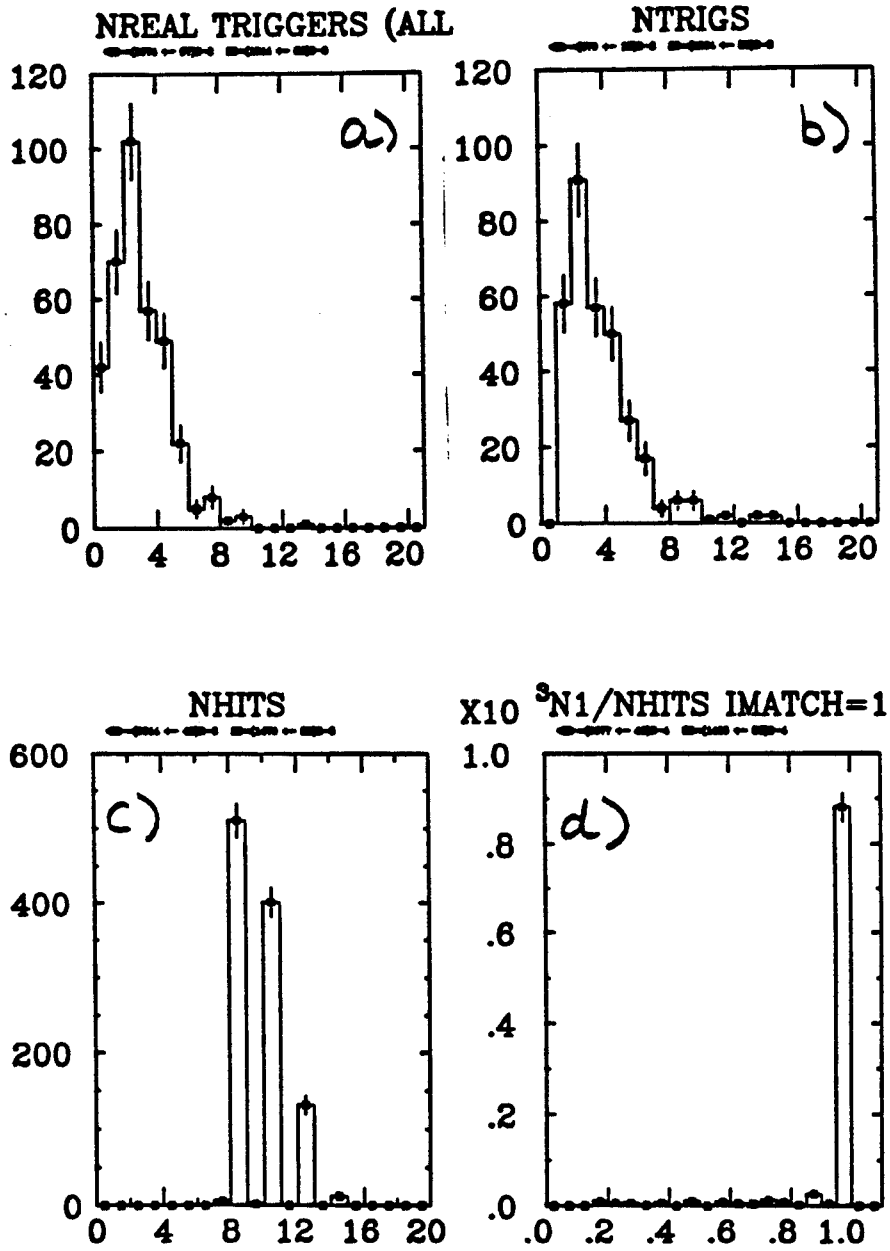


Figure 10 Forward silicon trigger studies for 800 GeV Higgs events at the SSC; the P_t threshold was set to 20 GeV/c. The plots show: a) the number of tracks in the event with $1 < |\eta| < 2.5$ and $P_t > 20$ GeV/c, b) the number of high P_t triggers found in the forward silicon, c) the number of hits associated with the trigger track (where this was required to be 7 or greater), d) the fraction of these hits that came from the same (Monte Carlo) track.

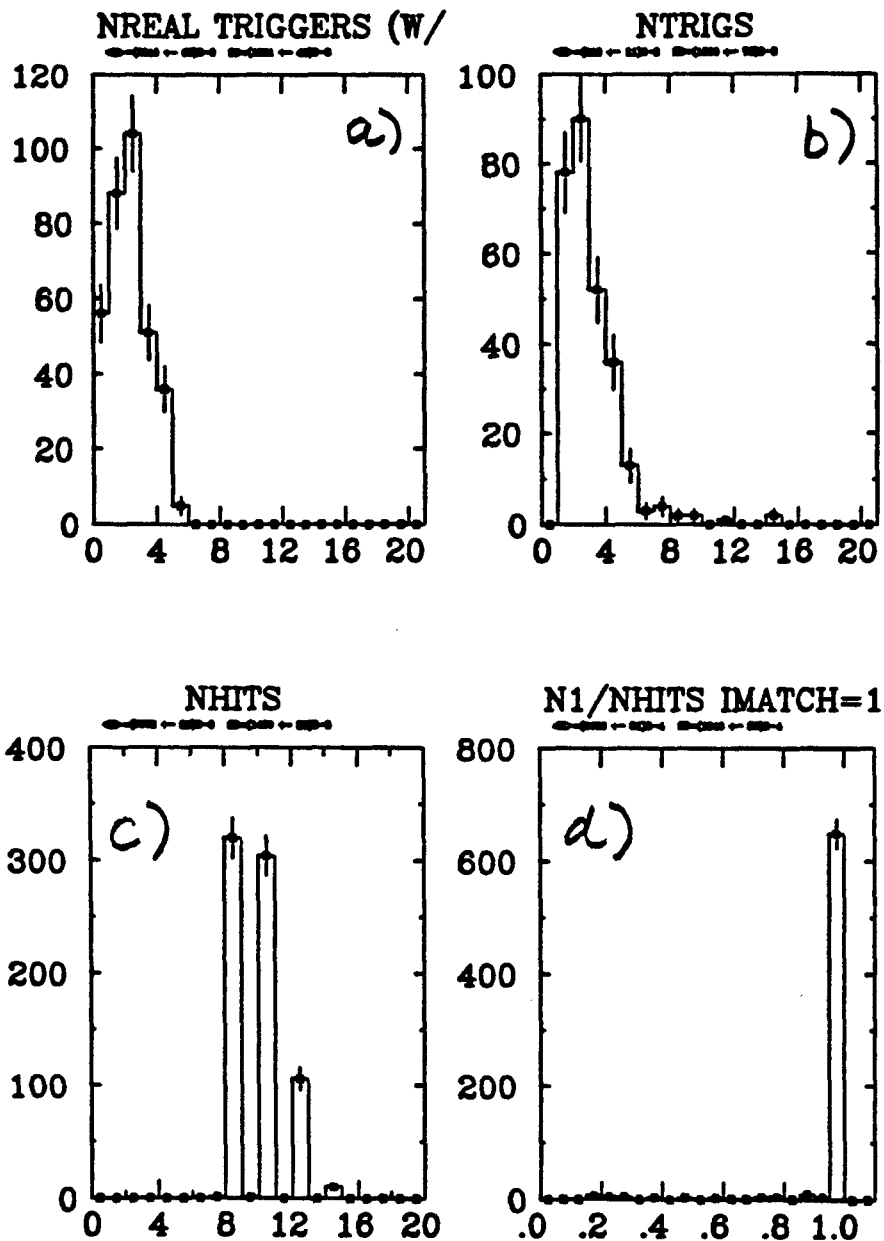


Figure 11 Forward silicon trigger studies for 800 GeV Higgs events at the SSC; the P_t threshold was set to 20 GeV/c, and the silicon triggers were required to be within ± 100 millirad of 10 GeV/c P_t threshold electromagnetic/muon triggers. The plots show: a) the number of leptons in the event with $1 < |\eta| < 2.5$ and $P_t > 20$ GeV/c, b) the number of high P_t triggers found in the forward silicon and agreeing with high P_t em/muon tracks, c) the number of hits associated with the trigger track (where this was required to be 7 or greater), d) the fraction of these hits that came from the same (Monte Carlo) track.